

สัญญาเลขที่ RSA5780057

รายงานวิจัยฉบับสมบูรณ์

โครงการบทบาทของไมโทฟาจี และการแสดงออกของโรคทางพันธุกรรมไมโทคอนเดรีย

ผู้วิจัย อ.นพ.ดร.ชยานนท์ พิระพิทยมงคล และคณะ

สังกัด คณะแพทยศาสตร์ศิริราชพยาบาล มหาวิทยาลัยมหิดล

สนับสนุนโดยสำนักงานกองทุนสนับสนุนการวิจัย

(ความเห็นในรายงานนี้เป็นของผู้วิจัย สกว. ไม่จำเป็นต้องเห็นด้วยเสมอไป)

## กิตติกรรมประกาศ

โครงการวิจัยครั้งนี้ได้รับการสนับสนุนจาก สกว. และได้รับความร่วมมือจากบุคคลต่างๆ อาทิ เช่น  
อาสาสมัครที่อุทิศเซลล์สร้างเส้นใยเพื่อประโยชน์ในการวิจัย ศ.พญ.ดร.พัชรีย์ เลิศฤทธิ์ ที่กรุณาให้คำแนะนำ และ  
สนับสนุนการวิจัยครั้งนี้ในเรื่องตัวอย่างเซลล์จากผู้ป่วย

นอกจากนี้ยังได้รับแรงบันดาลใจ กำลังใจในการทำงานจากนักศึกษาบัณฑิตในภาควิชาชีวเคมี ตลอดจน  
คณาจารย์และเพื่อนร่วมงานในภาควิชาชีวเคมี ภาควิชาตจวิทยา และภาควิชาเภสัชวิทยา และครอบครัว

ผู้วิจัย

อ.นพ.ดร.ชยานนท์ พิระพิทยมงคล

**Project Code : RSA5780057**

**Project Title : Study of the mitophagic activity in individual fibroblasts carrying the homoplasmic m.11778G>A mutation of Thai patients with Leber's hereditary optic neuropathy (LHON) disease**

**Investigator :Dr. Chayanon Peerapittayamongkol, Faculty of Medicine Siriraj Hospital, Mahidol University**

**E-mail Address : [Chayanon.pee@mahidol.ac.th](mailto:Chayanon.pee@mahidol.ac.th)**

**Project Period : 3 years**

This research is focused on three main important but related aspects of mitochondria—the powerhouse organelles residing in the cell with their own genetic materials. First, the balance of interconnected network vs fragmented forms of mitochondria is adaptable to metabolic need, development and stress conditions. Perturbation in this balance is likely ensuing the next aspect. Second, bioenergetics—keeping the proton gradient across inner membrane reflecting mitochondrial potential is the signature of healthy mitochondria and adequate supply of cellular energy in the form of ATP. Third, quality control of mitochondria—the process of recognition of damaged mitochondria and proper removal by lysosomal degradation of the whole organelle, namely mitophagy. Using a rare heritable form of blindness, namely Leber's hereditary optic neuropathy (LHON), as a model, we ask the question whether the three aspects related to mitochondria involve in the expression of disease or not. The basis of LHON disease is the mutation in the genetic material inside the organelle. Even though, all cells are full of mitochondria with the mutation—there is only 50% chance of developing the disease in male and to a lesser extent in female. The three aspects of mitochondria are also the mainstay of many age-related diseases in nowadays Thai society e.g. Alzheimer disease, Parkinson disease as well as cardiovascular disorders. With the advent of automated optic system plus image analysis software, unbiased-measurement of mitochondrial fission, membrane potential and quality control are emerged as important key not only to study the disease mechanism but also the for drug screening. Here, we reported using the three aspects of mitochondria to answer the question on disease expression in LHON. There are more than one mechanisms to prevent or to get the disease of course. One of the mechanism we uncover is the mitophagy. In one family, the patient who already develop the disease seemed to have limited ability to get rid of damaged mitochondria while his relative had higher levels of mitophagic activity resulting borderline energetic status.

**Keywords : LHON, mitophagy, mitochondrial membrane potential**

สัญญาเลขที่ : RSA5780057

ชื่อโครงการ : โครงการบทบาทของไมโทฟาจี และการแสดงออกของโรคทางพันธุกรรมไมโทคอนเดรีย

ชื่อผู้วิจัย : อ.ดร.นพ.ชยานนท์ พิระพิทยมงคล ภาควิชาชีวเคมี คณะแพทยศาสตร์ศิริราชพยาบาล มหาวิทยาลัยมหิดล

E-mail Address : Chayanon.pee@mahidol.ac.th

Project Period : 3 ปี

การวิจัยในครั้งนี้มุ่งเป้าไปทางคุณลักษณะสามอย่างที่เกี่ยวข้องกันของไมโทคอนเดรีย ที่เป็นออร์แกเนลล์ที่สำคัญของเซลล์เพราะเป็นแหล่งผลิตพลังงาน และมีสารกำหนดพันธุกรรมเป็นของตัวเอง ประการแรก สมดุลของภาวะที่ไมโทคอนเดรียเชื่อมต่อกันเป็นโครงข่าย และภาวะที่แตกหักเป็นท่อนสั้นๆ โดยสมดุลนี้สามารถปรับเปลี่ยนไปตามความต้องการของเมแทบอลิซึมของเซลล์ การเจริญเติบโต และตอบสนองต่อภาวะเครียด การรบกวนสมดุลนี้อาจส่งผลต่อไมโทคอนเดรียในเรื่องของชีวพลังงาน ในส่วนของการกักเก็บโปรตอนไว้ด้านนอกของเยื่อหุ้มชั้นในไมโทคอนเดรีย สามารถวัดได้เป็นความต่างศักย์ทางไฟฟ้าที่บ่งบอกถึงสุขภาพที่ดีของไมโทคอนเดรีย และศักยภาพในการสังเคราะห์พลังงานในรูปของ ATP ประการที่สามคือกระบวนการกำจัด และกำจัดไมโทคอนเดรียที่เสียหาย และนำส่งไปทำลายโดยไลโซโซมต่อไป กระบวนการกำจัดไมโทคอนเดรียนี้เราเรียกว่าไมโทฟาจี การวิจัยนี้ศึกษาโรคตาบอดทางพันธุกรรมที่เรียกว่าลอน โดยเน้นที่คุณลักษณะทั้งสามประการของไมโทคอนเดรีย และความสัมพันธ์กับการแสดงออกของโรค สาเหตุของโรคตาบอดพันธุกรรมลอนเกิดจากการกลายพันธุ์ของดีเอ็นเอภายในไมโทคอนเดรียเอง ถึงแม้ว่าไมโทคอนเดรียทุกอันในเซลล์เป็นไมโทคอนเดรียที่มีการกลายพันธุ์ทั้งหมดก็ตาม โอกาสของการเป็นโรคตาบอดนั้นมีอยู่ราวร้อยละ 50 ในผู้ชาย และโอกาสจะลดลงอีกในผู้หญิง ถึงแม้จะเป็นโรคที่พบได้ไม่บ่อยนักก็ตาม แต่กลไกที่เกี่ยวข้องกับทั้งสามคุณลักษณะของไมโทคอนเดรีย นั้นสามารถประยุกต์ไปใช้กับโรคต่างๆ ที่เกี่ยวข้องกับอายุมากขึ้นสำหรับสังคมผู้สูงอายุที่ประเทศไทยเข้าสู่อย่างเต็มตัวในปัจจุบันเช่น โรคอัลไซเมอร์ โรคพาร์กินสัน และโรคเกี่ยวกับหลอดเลือดหัวใจอุดตัน ด้วยการมาของเทคโนโลยีกล้องจุลทรรศน์ฟลูออเรสเซนซ์แบบอัตโนมัติ ประกอบกับโปรแกรมคอมพิวเตอร์ในการวิเคราะห์รูปภาพ เอื้ออำนวยให้เราสามารถพัฒนาการวัดการแตกหักเป็นท่อนของไมโทคอนเดรีย การวัดความต่างศักย์ทางไฟฟ้าของเยื่อหุ้มชั้นในของไมโทคอนเดรีย การวัดไมโทฟาจี ในลักษณะที่ปราศจากความลำเอียงของผู้ถ่ายภาพ การศึกษาคุณลักษณะสำคัญสามประการของไมโทคอนเดรีย เอื้ออำนวยให้ผู้วิจัยสามารถไขปัญหาการแสดงออกของโรคตาบอดลอน โดยกลไกหนึ่งที่ค้นพบคือข้อจำกัดของกระบวนการไมโทฟาจีอาจจะนำไปสู่การแสดงออกของโรค อันสืบเนื่องมาจากการสะสมของไมโทคอนเดรียที่ผิดปกติ หรือในอีกแง่หนึ่งการสนับสนุนไมโทฟาจีอย่างมีประสิทธิภาพอาจจะช่วยป้องกันการแสดงออกของโรคได้นั่นเอง

Keyword: โรคตาบอดพันธุกรรมลอน, ไมโทฟาจี, ความต่างศักย์ทางไฟฟ้าของไมโทคอนเดรีย

**Title: Study of the mitophagic activity in individual fibroblasts carrying the homoplasmic m.11778G>A mutation of Thai patients with Leber's hereditary optic neuropathy (LHON) disease**

**Objectives:**

1. Determination of mitophagic response of fibroblasts obtained from affected and unaffected individuals carrying homoplasmic m.11778G>A.
2. Generation of iPSCs from fibroblasts obtained from affected and unaffected individuals.
3. Induction of retinal ganglion cell/or neuronal progenitor cells differentiated from iPSCs
4. Assessment of differential mitophagic response between affected and unaffected neuronal cells together with their mitochondrial health status.

Induction of iPS was done without any success; therefore, the objectives were reduced to determination of mitophagic response of fibroblasts obtained from affected and unaffected individuals carrying homoplasmic m.11778G>A.

**Executive summary (English)**

This research is focused on three main important but related aspects of mitochondria—the powerhouse organelles residing in the cell with their own genetic materials. First, the balance of interconnected network vs fragmented forms of mitochondria is adaptable to metabolic need, development and stress conditions. Perturbation in this balance is likely ensuing the next aspect. Second, bioenergetics—keeping the proton gradient across inner membrane reflecting mitochondrial potential is the signature of healthy mitochondria and adequate supply of cellular energy in the form of ATP. Third, quality control of mitochondria—the process of recognition of damaged mitochondria and proper removal by lysosomal degradation of the whole organelle, namely mitophagy.

Using a rare heritable form of blindness, namely Leber's hereditary optic neuropathy (LHON), as a model, we ask the question whether the three aspects related to mitochondria involve in the expression of disease or not. The basis of LHON disease is the mutation in the genetic material inside the organelle. Even though, all cells are full of mitochondria with the mutation—there is only 50% chance of developing the disease in male and to a lesser extent in female. The three aspects of mitochondria are also the mainstay of many age-related diseases in nowadays Thai society e.g. Alzheimer disease, Parkinson disease as well as cardiovascular disorders.

With the advent of automated optic system plus image analysis software, unbiased-measurement of mitochondrial fission, membrane potential and quality control are emerged as important key not only to study the disease mechanism but also the for drug screening. Here, we reported using the three aspects of

mitochondria to answer the question on disease expression in LHON. There are more than one mechanisms to prevent or to get the disease of course. One of the mechanism we uncover is the mitophagy. In one family, the patient who already develop the disease seemed to have limited ability to get rid of damaged mitochondria while his relative had higher levels of mitophagic activity resulting borderline energetic status.

### **Executive summary (ภาษาไทย)**

การวิจัยในครั้งนี้มุ่งเป้าไปทางคุณลักษณะสามอย่างที่เกี่ยวข้องกันของไมโทคอนเดรีย ที่เป็นอแกเนลล์ที่สำคัญของเซลล์เพราะเป็นแหล่งผลิตพลังงาน และมีสารกำหนดพันธุกรรมเป็นของตัวเอง ประการแรก สมดุลของภาวะที่ไมโทคอนเดรียเชื่อมต่อกันเป็นโครงข่าย และภาวะที่แตกหักเป็นท่อนสั้นๆ โดยสมดุลนี้สามารถปรับเปลี่ยนไปตามความต้องการของเมแทบอลิซึมของเซลล์ การเจริญเติบโต และตอบสนองต่อภาวะเครียด การรบกวนสมดุลนี้อาจส่งผลต่อไมโทคอนเดรียในเรื่องของชีวพลังงาน ในส่วนของการกักเก็บโปรตอนไว้ด้านนอกของเยื่อหุ้มชั้นในไมโทคอนเดรีย สามารถวัดได้เป็นความต่างศักย์ทางไฟฟ้าที่บ่งบอกถึงสุขภาพที่ดีของไมโทคอนเดรีย และศักยภาพในการสังเคราะห์พลังงานในรูปของ ATP ประการที่สามคือกระบวนการกำจัด และกำจัด ไมโทคอนเดรียที่เสียหาย และนำส่งไปทำลายโดยไลโซโซมต่อไป กระบวนการกำจัดไมโทคอนเดรียนี้เราเรียกว่าไมโทฟาจี

การวิจัยนี้ศึกษาโรคตาบอดทางพันธุกรรมที่เรียกว่าลอน โดยเน้นที่คุณลักษณะทั้งสามประการของไมโทคอนเดรีย และความสัมพันธ์กับการแสดงออกของโรค สาเหตุของโรคตาบอดพันธุกรรมลอนเกิดจากการกลายพันธุ์ของดีเอ็นเอภายในไมโทคอนเดรียเอง ถึงแม้ว่าไมโทคอนเดรียทุกอันในเซลล์เป็นไมโทคอนเดรียที่มีการกลายพันธุ์ทั้งหมดก็ตาม โอกาสของการเป็นโรคตาบอดนั้นมีอยู่ราวร้อยละ 50 ในผู้ชาย และโอกาสจะลดลงอีกในผู้หญิง ถึงแม้จะเป็นโรคที่พบได้ไม่บ่อยนักก็ตาม แต่กลไกที่เกี่ยวข้องกับทั้งสามคุณลักษณะของไมโทคอนเดรียนั้นสามารถประยุกต์ไปใช้กับโรคต่างๆ ที่เกี่ยวข้องกับอายุมากขึ้นสำหรับสังคมผู้สูงอายุที่ประเทศไทยเข้าสู่อย่างเต็มตัวในปัจจุบันเช่น โรคอัลไซเมอร์ โรคพาร์กินสัน และโรคเกี่ยวกับหลอดเลือดหัวใจอุดตัน

ด้วยการมาของเทคโนโลยีกล้องจุลทรรศน์ฟลูออเรสเซนซ์แบบอัตโนมิติ ประกอบกับโปรแกรมคอมพิวเตอร์ในการวิเคราะห์รูปภาพเอื้ออำนวยให้เราสามารถพัฒนาการวัดการแตกหักเป็นท่อนของไมโทคอนเดรีย การวัดความต่างศักย์ทางไฟฟ้าของเยื่อหุ้มชั้นในของไมโทคอนเดรีย การวัดไมโทฟาจี ในลักษณะที่ปราศจากความลำเอียงของผู้ถ่ายภาพ การศึกษาคุณลักษณะสำคัญสามประการของไมโทคอนเดรียเอื้ออำนวยให้ผู้วิจัยสามารถไขปัญหาการแสดงออกของโรคตาบอดลอน โดยกลไกหนึ่งที่ค้นพบคือข้อจำกัดของกระบวนการไมโทฟาจีอาจจะนำไปสู่การแสดงออกของโรค อันสืบเนื่องมาจากการสะสมของไมโทคอนเดรียที่ผิดปกติ หรือในอีกแง่หนึ่งการสนับสนุนไมโทฟาจีอย่างมีประสิทธิภาพอาจจะช่วยป้องกันการแสดงออกของโรคได้นั่นเอง

## Background

LHON is an inherited central vision loss, caused by mitochondrial DNA mutation and transmitted by maternal pattern (non-Mendelian). The common mutations take place in nucleotide position 3460 (G->A) (1), 11778 (G->A) (2) and 14484 (T->C) (3) affecting subunits of complex I. Typical phenotype of LHON patient is visual loss in one eye without pain and the other eye can be affected almost simultaneously in nearly 50% of the patients (4, 5). The disease is characterized by male preponderance and incomplete penetrance (6).

One feature indicating healthy mitochondria is mitochondrial membrane potential (MMP or  $\Delta\Psi_m$ ), a value reflecting status of proton gradient between the matrix and intermembrane space of mitochondrion. During electron transport, Proton pumping via complexes I, III, and IV takes place directionally from the matrix into the intermembrane space. Subsequently, proton flows back through complex V and drives ATP synthesis Figure 1.

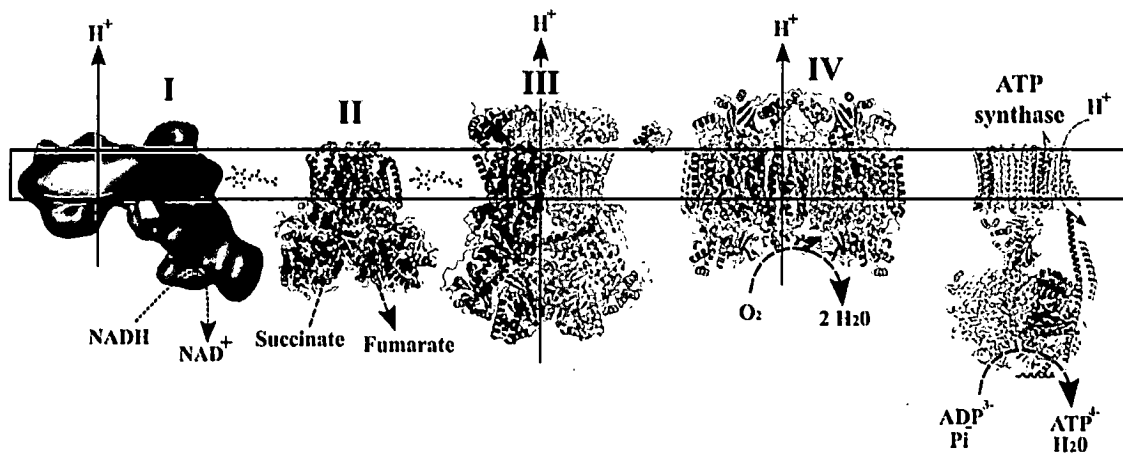


**Figure 1.** Electron transport chain and ATP synthase from (7).

Dissipation of MMP (during mitochondrial damage) causes accumulation of PTEN-induced kinase 1 (PINK1) on the outer membrane of mitochondria leading to initiation of autophagophore through activation of unc-51-like kinase (ULK1/2) (8). The conversion of microtubule-associated protein 1A/1B-light chain 3 (LC3-I) to LC3-II (LC3-phosphatidylethanolamine conjugate) by uncharacterized human autophagy-related (ATG) gene product counterparts. Phagophore-associated LC3-IIs embrace PARKIN-coated mitochondrion and finally form the autophagosome. Autophagosome fuses with lysosome becoming autophagolysosome and components after digestion are recycled.

The equivalent of human LHON mutations in mutagenized mouse cell lines reproducibly cause mitochondrial dysfunctions, such as reduced MMP and ATP

synthesis and increased ROS production.(9) However, defective in ATP production was not consistently reported among LHON patients. (10, 11)

## **Materials and methods**

### **Samples**

Fibroblast cells were maintained from skin biopsies derived from male subjects: 3 from healthy control, 3 unaffected carriers and 3 patients carrying homoplasmic m.11778G>A mutation. Two affected LHON patients (A1, A2) and two unaffected carriers (U1, U2) were recruited from family 79 and the other affected LHON (A3) and unaffected carrier (U3) were from family 1 (provided by Prof. Dr. Patcharee Lertrit).

### **Fibroblast culture**

Fibroblasts were maintained in Dulbecco's modified Eagle medium (DMEM, 5 mM glucose, Gibco) supplemented with 10% fetal bovine serum, amphotericin B (1 µg/mL, penicillin (100 U/mL) and streptomycin (100 µg/mL). The culture conditions were 5%CO<sub>2</sub> at 37°C with media replacement every other day.

For induction of mitophagy, carbonyl cyanide *p*-(trifluoromethoxy)-phenylhydrazone (FCCP, Sigma-Aldrich), a popular and efficient mitochondrial uncoupler (12), was mixed in media at the concentration of 10 µM with or without chloroquine (various concentrations, Sigma-ALdrich) to inhibit autophagic flux (13).

### **Western blot analysis of LC3-I/LC3-II conversion**

Fibroblast lysates were prepared, separated on 15-20% gel (SDS-PAGE), transferred to nitrocellulose membrane and incubated against anti-LC3B antibody (1:1,000; NB600-1384, Novus Biologicals) or anti-citrate synthetase antibody (1:5,000; ab129088, Abcam) as loading control. Anti-rabbit IgG VHH single domain (conjugated with Horseradish peroxidase) antibody (1:20,000, ab191866, Abcam) was used as secondary antibody. Protein bands were imaged under ImageQuant LAS 4010 system (GE Healthcare).

Figure 2 showed typical results of immunoblots.



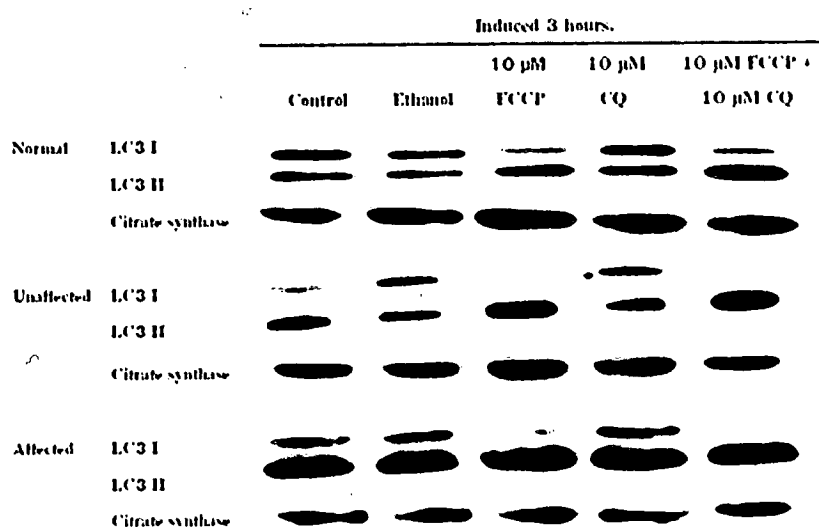


**Figure 2.** Western blot of fibroblast lysate reacted with anti-LC3 antibody and anti-citrate synthase antibody as loading controls after treatment with 10 μM FCCP with or without 10 μM chloroquine.

Unlike conventional, we used ratios of LC3B-II/LC3B-I + LC3B-II to represent autophagic activity. This formula was less sensitive to the decrement of LC3B-I upon activation. There were 3 subjects in normal control, unaffected carriers and affected and the experiments were done in 3 independent replicates. The overall results were plotted in Figure 3. Two-way analysis of variance was performed with sample groups vs treatments using statistical software, Jamovi 0.9.6.1 (obtained free from <https://www.jamovi.org>) and was shown in **Table 1,2**.

**Table 1** Two-way ANOVA test of sample groups and treatments on LC3B ratios.

ANOVA					
	Sum of Squares	df	Mean Square	F	p
Sample	0.867	2	0.433	20.271	< .0001
Treatment	6.716	4	1.679	78.521	< .0001
Sample * Treatment	0.364	8	0.046	2.129	0.0380
Residuals	2.566	120	0.021		

There were statistically significant differences of both sample groups and treatments on autophagic activity in fibroblasts.

**Table 2** Post hoc comparisons between sample groups.

Post Hoc Comparisons - Sample						
Comparison		Mean Difference	SE	df	t	ptukey
Sample	Sample					
N	- U	-0.067	0.031	120.000	-2.179	0.0789
	- A	-0.193	0.031	120.000	-6.271	< .0001
U	- A	-0.126	0.031	120.000	-4.092	0.0002

There were significant increase in autophagic activity in fibroblasts from affected group when compared either to normal control or to unaffected carriers. However, there was a tendency of higher autophagy in unaffected fibroblasts when compared to normal control but this was not statistically significant.

**Table 3** Post hoc comparison between treatments.

Post Hoc Comparisons - Treatment						
Comparison		Mean Difference	SE	df	t	ptukey
Treatment	Treatment					
Water	- EtOH	-0.006	0.040	120.000	-0.145	0.9999
	- FCCP	-0.465	0.040	120.000	-11.686	< .0001
	- CQ	-0.202	0.040	120.000	-5.086	< .0001
	- FQ	-0.530	0.040	120.000	-13.322	< .0001
EtOH	- FCCP	-0.459	0.040	120.000	-11.541	< .0001
	- CQ	-0.197	0.040	120.000	-4.941	< .0001
	- FQ	-0.524	0.040	120.000	-13.177	< .0001
FCCP	- CQ	0.263	0.040	120.000	6.600	< .0001
	- FQ	-0.065	0.040	120.000	-1.636	0.4777
CQ	- FQ	-0.328	0.040	120.000	-8.236	< .0001

Water=untreated; EtOH=ethanol as vehicle control; FCCP=treatment with 10  $\mu$ M FCCP; CQ=treatment with 10  $\mu$ M chloroquine and FQ=treatment with 10  $\mu$ M FCCP plus 10  $\mu$ M chloroquine.

From Table 3, there were significant increase in LC3B-II in response to both FCCP or chloroquine alone and FCCP plus chloroquine. There were no changes in LC3B-II in untreated group and vehicle control as well as treatment with FCCP alone or in combination with chloroquine. The interaction term between sample group and treatment which was statistically significant in two-way ANOVA test (Table 1) was due to special situation only in affected group. Treatment with chloroquine alone or FCCP alone cause no significant changes in LC3B-II conversion.

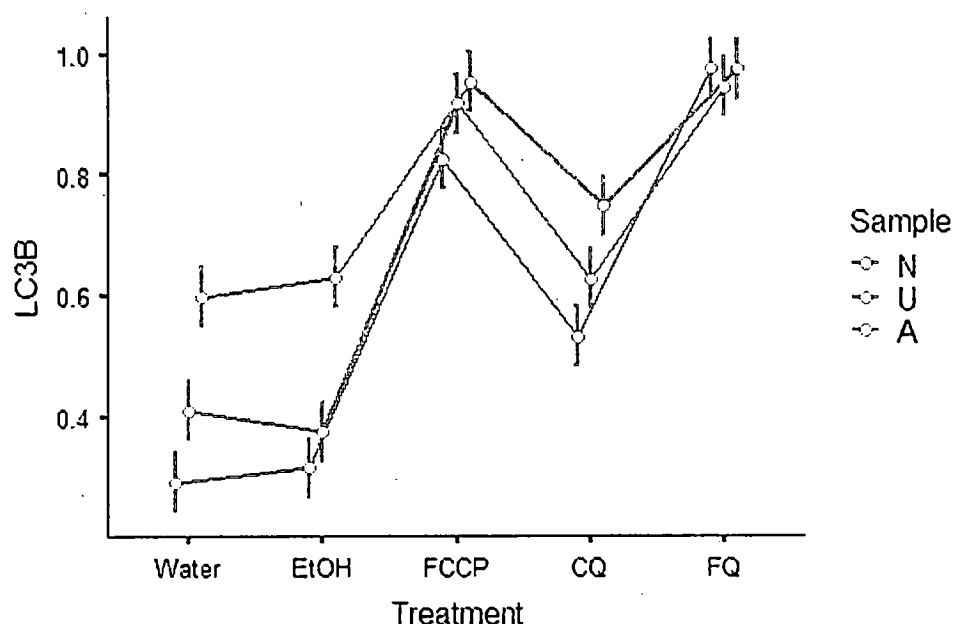


**Figure 3.** Bar plot of LC3BII conversion according to various treatments. (mean $\pm$ SEM)

Water=untreated; EtOH=ethanol as vehicle control; FCCP=treatment with 10  $\mu$ M FCCP; CQ=treatment with 10  $\mu$ M chloroquine and FQ=treatment with 10  $\mu$ M FCCP plus 10  $\mu$ M chloroquine.

### Study of ATP production

#### Method 1 Digitonin permeabilization

Fibroblasts at 80-90% confluency were trypsinized, washed twice with PBS and resuspended in respiratory buffer containing 100 mM KCl, 5 mM potassium phosphate, 1 mM EGTA, 3 mM EDTA, 10 mM Tris-HCl, pH 7.4). Digitonin permeabilization was performed at the final concentration of 25  $\mu$ g/mL (14, 15).

#### ATP measurement

ATP measurement was performed in ATP Bioluminescent Assay Kit (FLAA, Sigma-Aldrich) according to the manufacturer's protocol in the presence of 0.15 mM P<sub>1</sub>, P<sub>5</sub>-Di (adenosine-5') pentaphosphate and 4 mM ADP. Chemiluminescence was measured every 5-10 seconds on using multidetection microplate reader, Synergy H1(BioTek),

Figure 4 represented typically chemiluminescence measurement and mitochondria preserved capacity for ATP production in both carriers and affected groups.

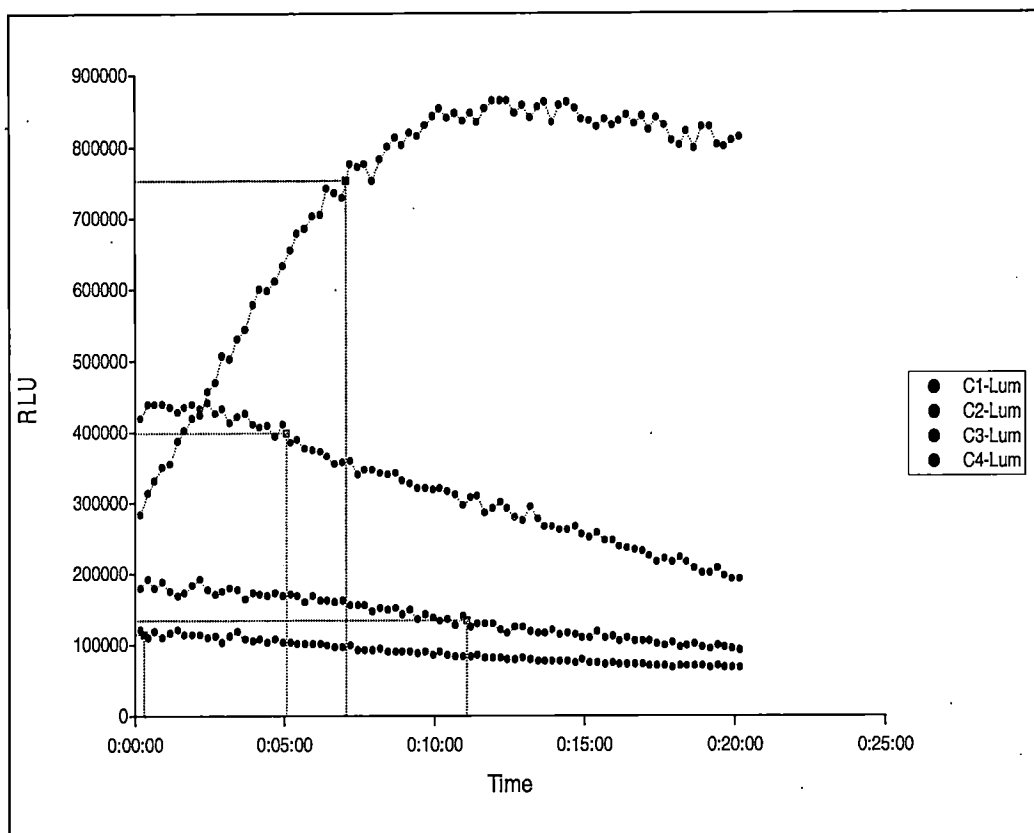


**Figure 4.** C1 complex I substrates added; C2 complex I substrates plus rotenone; C3 complex I substrates plus oligomycin and C4 no substrate added.

ATP production in the presence of complex I substrates was presented in Table 1.

**Table 4.** Results of complex I activity assayed by digitonin permeabilization method.

Status		Complex I
	name	glutamate and malate
		(nM ATP/min/ $10^5$ cells)
normal	N1	152.63
normal	N2	229.6184
normal	N3	194.2323
affected	A1	247.8223
affected	A2	311.4377
affected	A3	357.7669
unaffected	U1	180.9217

unaffected	U2	173.9326
unaffected	U3	51.9591

## Method 2 ATP content measurement

Using ATPlite 1 step (PerkinElmer) to measure cellular ATP content, we could evaluate cellular ATP content with more confidence because this method was devoid of any washing step.

Fibroblasts were seeded on 96-well tissue culture plate with cell number of 10,000 in each well for 18-24 h. After removal of media, the levels of ATP were measured by adding substrate solution 100  $\mu$ L/well, the plate was then shaken for 2 min at 20-22°C and the luminescence signals were detected with multi-detection microplate reader (USA/Synergy H1) within 30 minutes.

## Results

Mean ATP concentration for normal control was 1.89  $\mu$ M, for affected from family 79 was 2.03  $\mu$ M and for unaffected from family 79 was 1.87  $\mu$ M (n=2 for each group). In summary, there was no apparent reduction of cellular ATP in both unaffected and affected groups from family 79 which was consistent with mitochondrial membrane potential in the next study. We could not conduct the same measurement on subjects from family 1 because of budget limitation.

## Study of mitochondrial membrane potential (MMP)

Mitochondrial membrane potential (MMP) was assessed by MITO-ID® Membrane potential detection kit (Enzo Life Science) which is relied on dual-emission property of dye—in cytosol it is in monomeric state and emits green fluorescence while taken up into mitochondria in MMP dependent manner it is in aggregate form and emits orange fluorescence. Highly polarized mitochondria will therefore accumulate dye in aggregate form and fluoresces orange light. There was no obvious difference in orange fluorescence (indicating polarized mitochondria) among the three groups (normal, unaffected and affected). So, we needed stress conditions and image analysis to obtain quantitative values of polarized mitochondria.

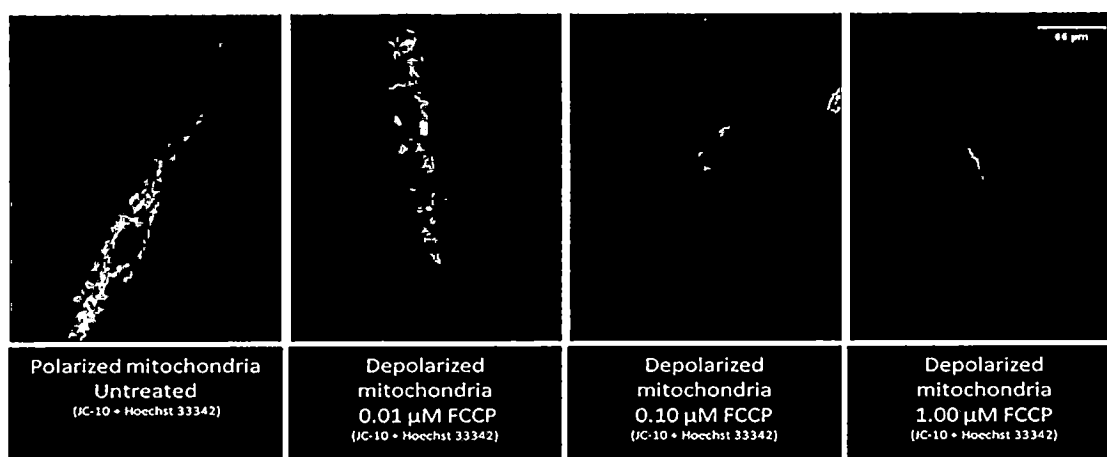


**Figure 5.** Demonstration of polarized mitochondria in fibroblasts taken with 20X. The decrease of orange fluorescence from left to right with increasing concentration of the protonophore: vehicle control, 0.01  $\mu\text{M}$ , 0.1  $\mu\text{M}$  and 1  $\mu\text{M}$  FCCP, respectively. Images taken from Operetta High-Content Imaging System (PerkinElmer).

Around 5,000 cells were seeded per well and incubated overnight. After being attached to the bottom of well, cells were stained by the MITO-ID® membrane potential dye (Enzo Life Science) [1:100] and Hoechst 33342 [1:1000] for 30 min and washed twice by the media. Cells were treated with FCCP in various concentration (0.01  $\mu\text{M}$ , 0.1  $\mu\text{M}$  and 1  $\mu\text{M}$ ) and with 0.2% ethanol as vehicle control for 1 h. Cells were observed under the Operetta CLS machine with the specific excitation and emission wavelengths. For FITC channel, samples were excited at 485 nm and measured emission at 530 nm (for rhodamine channel excited at 540 nm/emits at 570 nm and for nucleus channel (Hoechst 33342) excited at 350nm/emitted 461 nm). Figure 5 demonstrated the typical pictures of cell treated with increasing concentration of FCCP. The fluorescent data were analyzed by CellProfiler version 3.

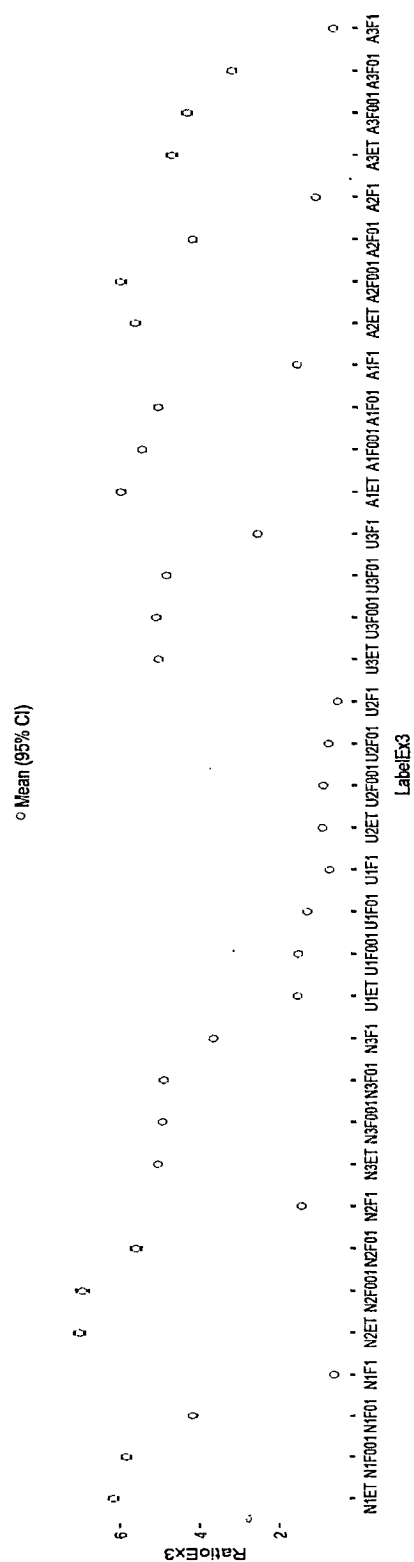


**Figure 6** Plots of ratios representing mitochondrial membrane potential (MMP) according to treatment and affected status. MMP was represented by mean $\pm$ 95% confidence interval.

It was really difficult to have primary fibroblast culture in the same confluency and healthy. The orange to green fluorescence representing MMP for 9 samples was shown in Figure 6. The sample U1 and U2 were not healthy judging from their low MMP even in the untreated condition. Apparently, the sample A1 and A2 exhibited MMP within normal values (N1,N2 and N3) while the sample U3 exhibited MMP close to borderline ( $\sim$ N3). Interestingly, the MMP of A3 was lower than normal range.

This notion was seen in independent experiment shown in Figure 7. In this experiment, there were only 4 samples: N1, U3, A1 and A3. In brief, MMP of U3 and A1 cells was not statistically different from that of N1 (for vehicle control). The MMP of sample A3 was statistically lower than that of N1 (p-value = 0.0017, Dwass-Steel-Critchow-Fligner (DSCF) pairwise comparison). The MMP of sample A3 was statistically lower than that of U3 (p-value=0.0004, DSCF pairwise comparison)

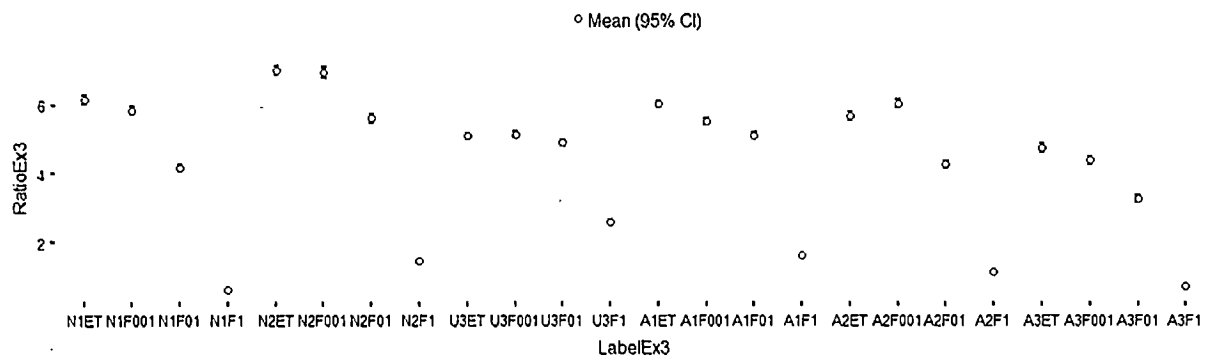


**Figure 7** Plots of ratios representing mitochondrial membrane potential (MMP) according to treatment and affected status in independent experiment from that in Figure 4. MMP was represented by mean $\pm$ 95% confidence interval.

ET=ethanol as vehicle control; F001=0.01  $\mu$ M FCCP; F01= 0.1  $\mu$ M FCCP; F1=1  $\mu$ M FCCP)

### Study of FCCP induced mitochondrial fragmentation

Validation of mitochondrial dye staining was done by first incubating fibroblasts with varying concentrations of FCCP from 1, 5 and 10  $\mu$ M for 3 h and subsequently stained with Mitochondrial Dye Red dye. Figure 8 demonstrated the dose-dependent morphological changes of mitochondrial network.



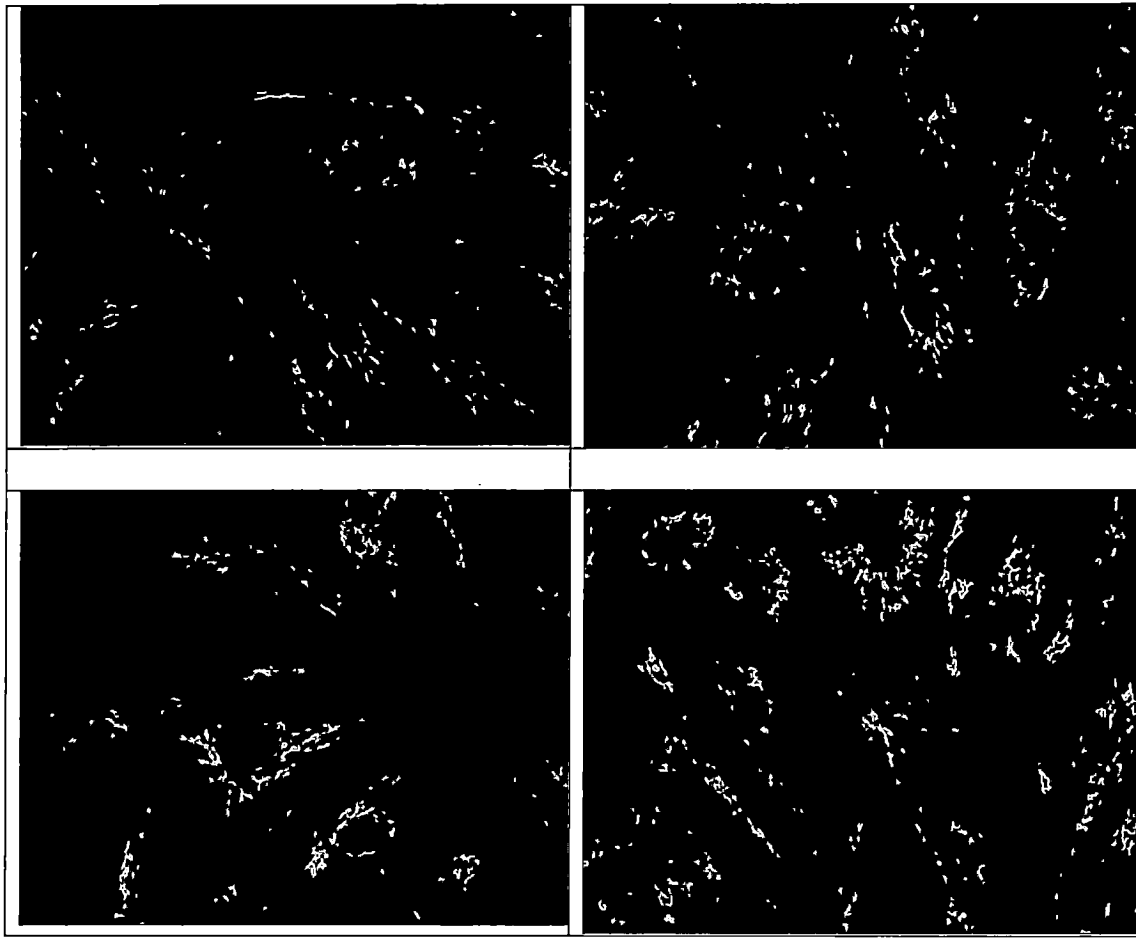


**Figure 8.** Upper left: untreated fibroblasts; upper right: fibroblasts treated with 1  $\mu$ M FCCP for 3 h; lower left: fibroblasts treated with 5  $\mu$ M FCCP for 3 h and lower right: fibroblasts treated with 10  $\mu$ M FCCP for 3 h.

Notably, there were shortening and fragmented mitochondria. The similar changes were observed for one LHON patient and his relative (data not shown). Further quantitative measurement of morphological changes is required to compare whether there are any differential responses to FCCP among subjects.

### Study of mitophagy

#### **Method 1** Colocalization of Cyto-ID green with mitochondrial marker (MitID red)

Before FCCP treatment, fibroblasts were maintained in DMEM supplemented with 10% FBS without phenol red. Cells were treated with 1  $\mu$ M FCCP for 6 h and

processed for Both CYTO-ID®, MITO-ID® and Hoechst counter staining as mentioned above.

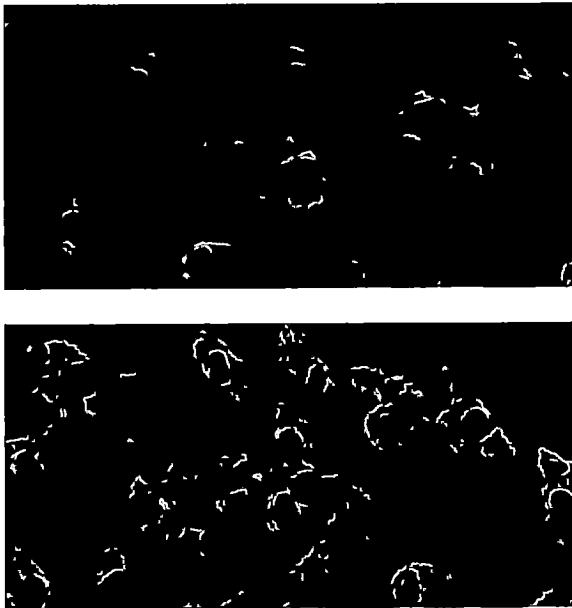


**Figure 9.** On the upper panel, cells treated with vehicle (ethanol, as FCCP dissolved in). On the lower, cells treated with 1  $\mu$ M FCCP for 6 h. Visualization was performed using wide field fluorescence microscope 20X. Background and fluorescence channel crossover were corrected using Spectral\_unmixing plugin in ImageJ version 1.49t.

## Results

Blue color represented the nuclei, red for mitochondrial network and green for autophagosome/autolysosome. Chemical dissipation of mitochondrial membrane potential caused impaired mitochondria which augmented the elimination of such mitochondria by autophagy as green color stained perinuclear regions in Figure 9 on the right hand side. Note that on the right figure, depolarized mitochondria were still brightly stained with MITO-ID red a bit more irregular pattern. Further work is needed to delineate and quantify the colocalization of red and green colors at higher magnification ( $\geq 60\times$ ).

Nonparametric multiple comparison was done and it turned out that only cells treated with 50  $\mu$ M chloroquine alone (compared with untreated) exhibited the significant colocalization of autophagosomes (CytolD green) and mitochondria (Mito-ID red) (P-value = 0.0004). None of the treatment with FCCP alone or with chloroquine up to 30  $\mu$ M concentrations gave statistical significant difference comparing with untreated.

## Method 2 Colocalization of GFP-LC3 with mitochondrial marker (MitoID red)

Lentiviral GFP-LC3, Lentibrite GFP-LC3 Lentiviral Biosensor, was purchased from Merck-Milipore. Fibroblast cells are grown to 50-70% confluency and then transduced with lentiviral particle with varying MOI (multiplicity of infection) 10-40. Infected fibroblasts were continued incubation for 24 h before being challenged with FCCP.

## Results

After transduction with Lentiviral GFP-LC3, fibroblasts were challenged with 1  $\mu$ M FCCP with or without 50  $\mu$ M chloroquine (lysosome inhibitor). Nuclei were stained with Hoechst and then visualized under wide field fluorescence microscope. Background correction and channel crossover unmixing were employed on images using ImagJ with Spectral\_Unmixing plugin Figure 10.

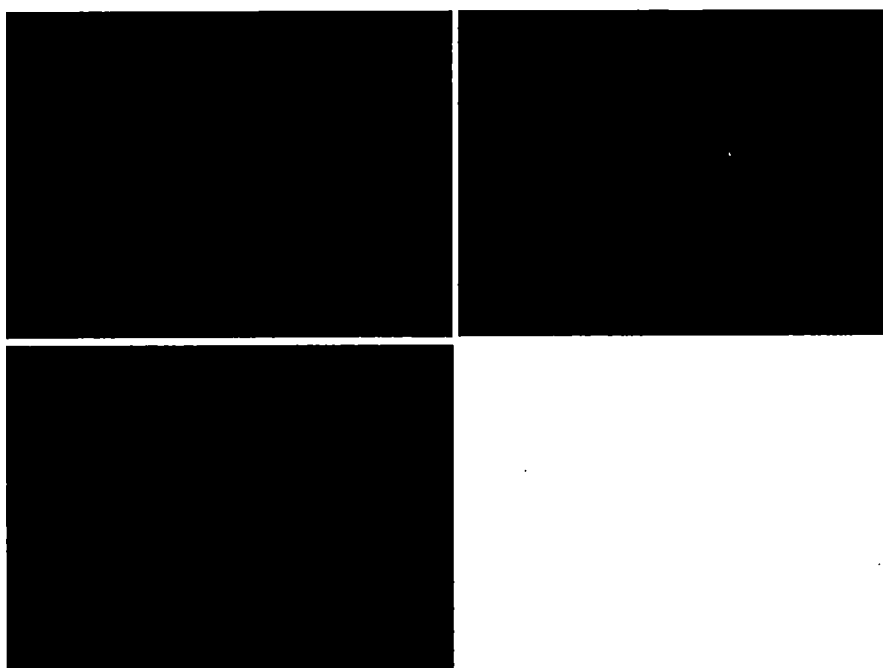


**Figure 10.** Upper left, control untreated cells (vehicle); Upper right, 1  $\mu$ M FCCP treated cells and Lower left, 1  $\mu$ M FCCP plus 50  $\mu$ M chloroquine.

No difference in GFP patterns among cells—vehicle, 1  $\mu$ M FCCP alone and 1  $\mu$ M FCCP with 50  $\mu$ M chloroquine was observed under 40X magnification. Lipidated GFP-LC3 II is expected to form punctate upon mitophagic induction.

## Method 3 Colocalization of Anti-LC3 antibody (antirabbit IgG conjugated with Alexa 488) with mitochondrial marker (MitoID® red)

We also failed to demonstrated mitophagy only with FCCP treatment but not with cloroquine (data not shown).

#### **Method 4** Delivery of mitochondria to lysosome using mKeima protein.

mKeima is modified protein from Keima protein (16)(15)(coral-derivative fluorescent protein). A mitochondria target sequence from COX8A (cytochrome c oxidase subunit 8A) was added to Keima in the plasmid. This expressed protein will localize to mitochondria with a change in excitation wavelength from 440 to 550 nm (emitted the same wave length at 660 nm) when it is delivered to lysosome (acid environment). The switching of excitation wavelength can be detected by Operetta imaging analyzer. mKeima-Red-Mito-7 plasmid is purchased from ADDGENE laboratory. This plasmid contains mKeima gene with mitochondrial tagged sequence under CMV (cytomegalovirus) promoter and kanamycin resistance gene for selection. The CMV promoter can be used by human cell.

#### **Harvesting mKeima plasmid**

Transformed non-pathogenic *E. coli* were cultured in kanamycin added LB agar and LB broth. LB agar is used for colony isolation and LB broth used for harvesting plasmid. We use Zymo PURE Midi Prep Kit or NucleoSpin kit for plasmid extraction. Nanophotometer was used to quantify the concentration of plasmid in solution.

#### **Transfection mKeima plasmid into cell**

Either lipofectamine or Amaxa™ 4D-Nucleofector™ were employed to enhance transfection of the mKeima plasmid into fibroblast cell. For lipofectamine protocol, fibroblast was grown to 80-90% confluency with media changed every 2 days to prevent cells from starvation that would stimulate autophagy. Rocking reverse transfection method was exploited by incubating lipofectamine and plasmid together and then transferred to cell solution. The culture was shaken at 60-80 rpm, 25°C. Then, the cell solution was seeded into the 96-well plate. The plate was kept for 10 minutes at room temperature before incubation at 37 °C. Visualization was observed under fluorescent image analyzer after 24-48 h post transfections. Alternatively, for transfection with Amaxa™ 4D-Nucleofector™ machine, P2 Primary Cell 4D-Nucleofector™ X Kit was chosen. The method were followed the manufacturer's manual with slight modifications.

#### **Verification of mKeima protein**

mKeima-Transfected fibroblast cell were verified by poring the cell with 0.05% triton-x in pH 4 (cytoplasm environment) and pH 7 (autophagolysosome environment) F12 media and capture fluorescent signal by Operetta program.

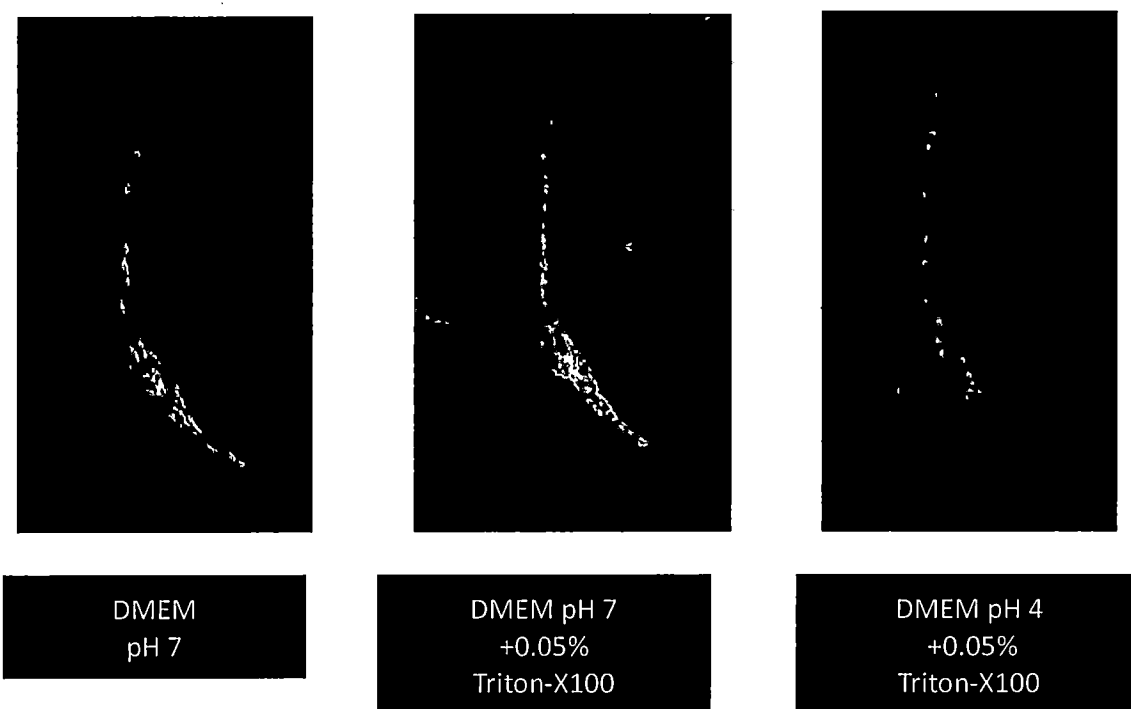


**Figure 11.** Fluorescence signals from mKeima protein expressed in fibroblast cell. Left: expression of mKeima in normal cell and captured with excitation wavelength of 440 (pseudo green color) and 550 nm (pseudo red color), noted network-like pattern consistent with mitochondrial network. Middle: Triton-X100 perforated cell in media with pH 7. Right: Triton-X100 perforated cell in media with pH 4.

mKeima protein was verified as indicator of mitochondrial delivery to lysosome. First, by permeabilization of fibroblast with Triton-X100 and the media was switched from pH 7 to pH 4 as in Figure 11. For normal control fibroblast cell, we observed the shifting of excitation wave length from 440 to 550 nm when cells were treated with 10 M FCCP for 8 h. However, this method was not amenable to through put study because of low intensity of the mKeima and low efficiency of transfection of mKeima plasmid to fibroblast.

**Method 5** Colocalization of mitochondrial specific dye (MITO-ID® red) with lysosome staining dye (Lysosome staining kit)

We stained fibroblast cells with MITO-ID® red (Enzo Life Sciences) (ex/em: 558/690 nm), and lysosome by Lysosome staining kit (Abcam) (ex/em: 490/525 nm) and Hoechst 33342 dye (ex/em: 350/461 nm) for 30 minutes. After staining, cells were observed under the Operetta CLS™ image analyser.

When fibroblast cells were exposed to 10  $\mu$ M FCCP for 6-8 h, mitochondrial network was disrupted and colocalization of mitochondria and lysosome as in Figure 12.

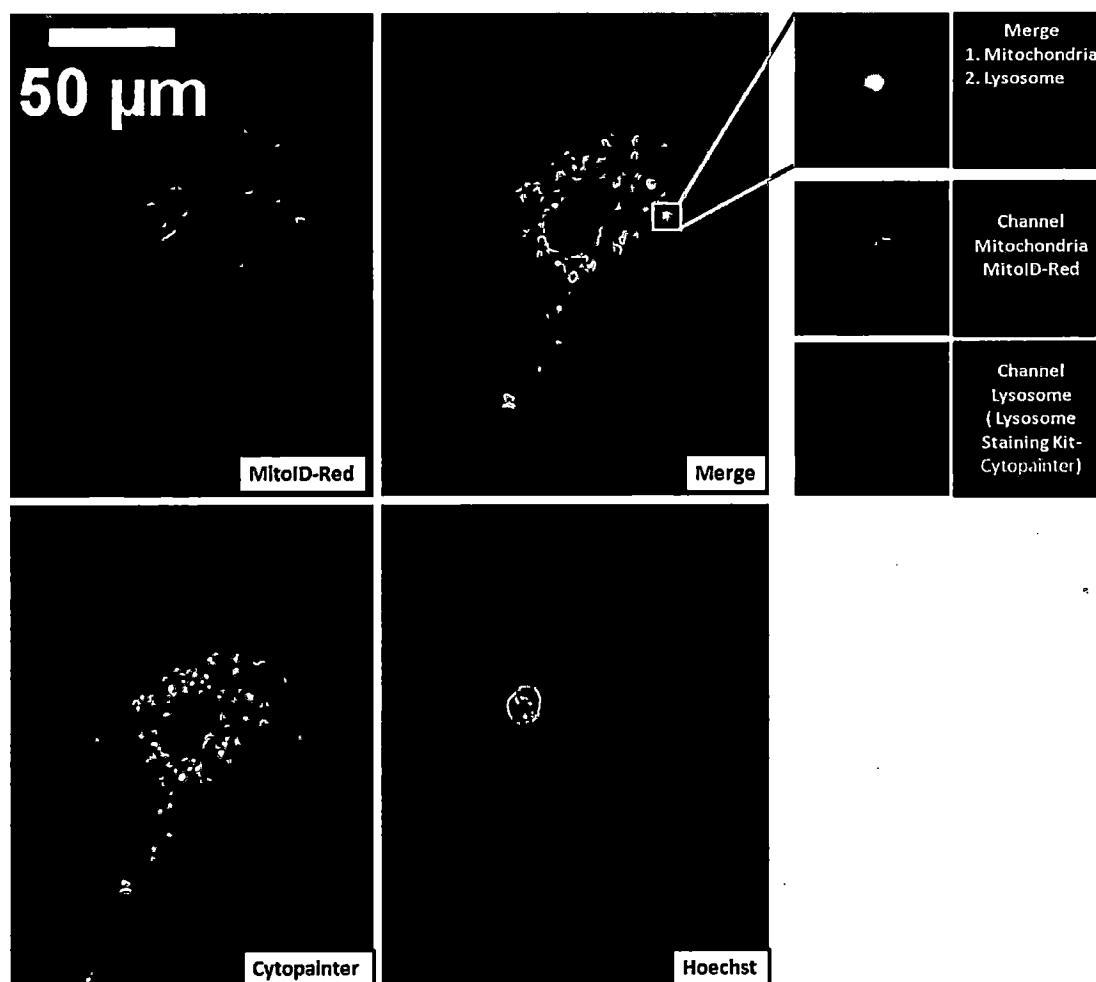


**Figure 12.** Demonstration of mitophagy by colocalization of mitochondrion and lysosome.

Mitophagy unit was calculated by ratios of colocalized mitochondria (with lysosome) divided by sum of colocalized and non-colocalized mitochondria in each cell by using CellProfiler program with the pipeline shown Table 5.

**Table 5** Pipeline for detection of mitophagy.

Analysis sequence of mitophagy events detection	
Set	Method
1	Input image and metadata extraction
2	Correction illumination Calculate and Apply

3	Identify primary object [Nucleus]
4	Measure object intensity and filter object
5	Identify secondary object [Mitochondria]
6	identify tertiary object [Cytoplasm]
7	Identify primary object [Mitochondria]
8	Identify primary object [Lysosome]
9	Expand Or Shink object [Mitochondria and Lysosome]
10	Relate Object [Cytoplasm – Mitochondria - Lysosome]
11	Classify Object [Colocalized and not colocalized]
12	Calculate math [Colocalized/(Colocalized+not Colocalized)]
13	Export to spread sheet

### Verification of mitophagic activity according to known inducer (FCCP).

Fibroblasts from normal control, unaffected and affected were treated with known mitophagic inducer—FCCP at the concentration of 10 M for 6-8 h and compared with 10  $\mu$ M chloroquine, vehicle control, respectively. Mitophagy unit was presented in Figure 13.

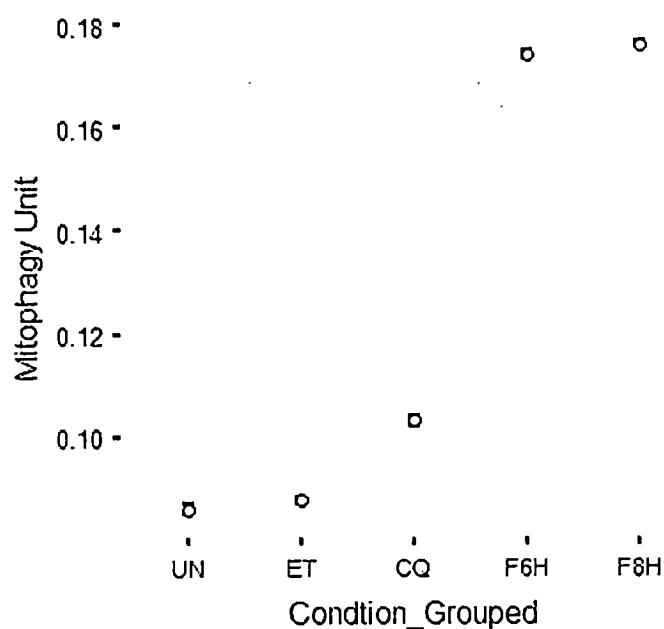


**Figure 13.** Mitophagy unit (represented by mean $\pm$ 95% confidence intervals) of all samples with UN (untreated), ET (ethanol as vehicle control), CQ (10  $\mu$ M chloroquine), F6H (10  $\mu$ M FCCP for 6 h) and F8H (10  $\mu$ M FCCP for 8 h).

For overall sample-wise responses to treatment were shown in Figure 14.

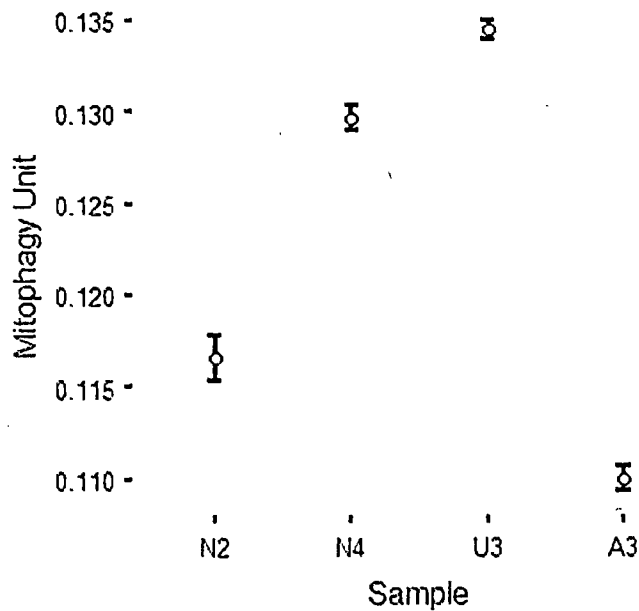


**Figure 14.** Overall response to treatment for normal control (N2, N4), unaffected (U3) and affected (A3). (represented by mean±95% confidence intervals)

Unexpectedly, unaffected LHON fibroblast (U3) showed highest basal (uninduced) mitophagy activity compared to normal control (U3 vs N2, p-values =  $1.41 \times 10^{-9}$ , U3 vs N3 3, p-values =  $1.41 \times 10^{-9}$ ) and compared to patient (U3 vs A3, p-value =  $1.41 \times 10^{-9}$ ) see Figure 14,15. With chloroquine treatment, all samples exhibited greater proportions of mitophagy suggesting that there were comparable degrees of lysosomal degradation. For induced mitophagy, patient's fibroblast still showed diminished mitophagy when compared to both unaffected and normal control (at 8 h).



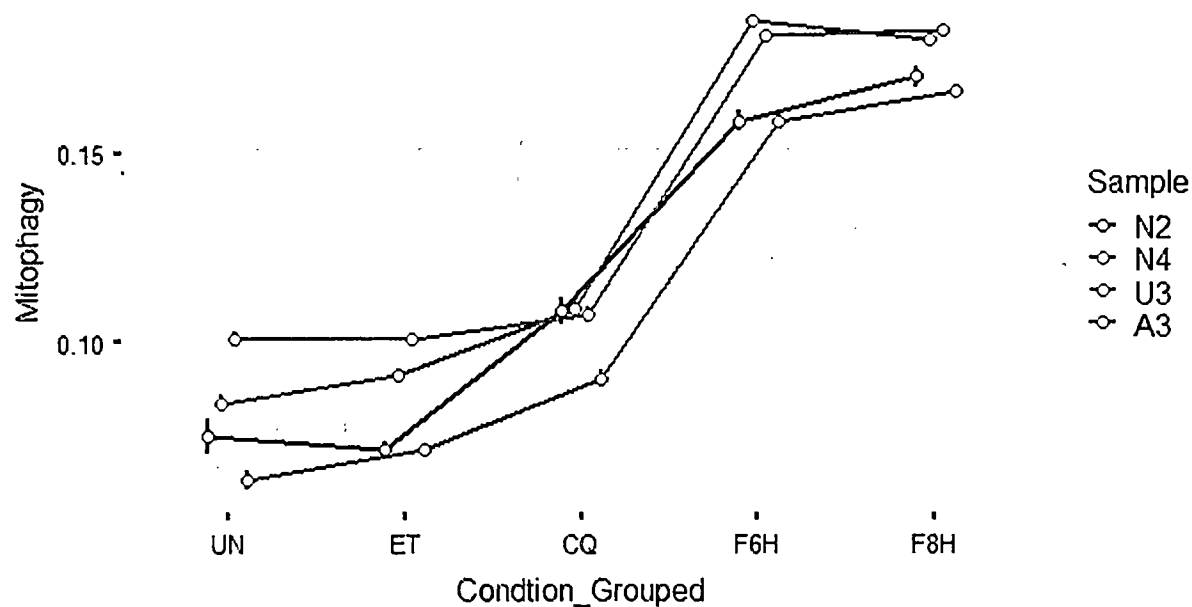


**Figure 15.** Mitophagy unit according to various treatments on X-axis and to each subject represented by separate lines. (represented by mean $\pm$ 95% confidence intervals)

UN (untreated), ET (ethanol as vehicle control), CQ (10  $\mu$ M chloroquine), F6H (10  $\mu$ M FCCP for 6 h) and F8H (10  $\mu$ M FCCP for 8 h)

An increase in mitophagic activity of U3 relative to A3 could be replicate in the other experiment shown in Figure 16.

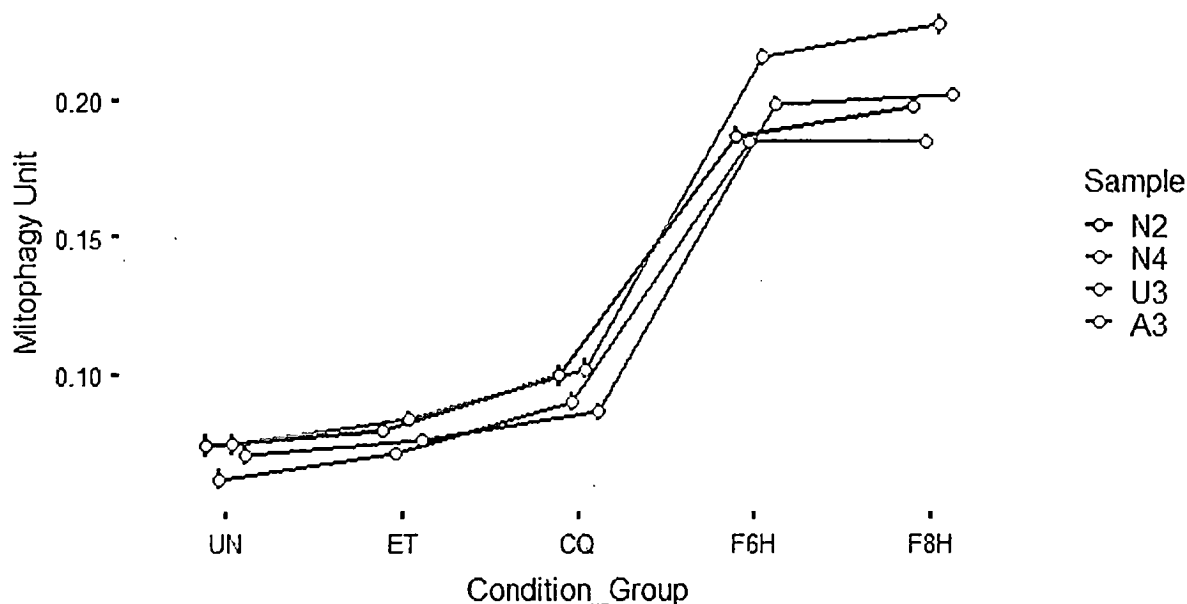


**Figure 16.** Mitophagy unit according to various treatments on X-axis and to each subject represented by separate lines (in separate experiment from that in Figure 13). (Represented by mean $\pm$ 95% confidence intervals)

UN (untreated), ET (ethanol as vehicle control), CQ (10  $\mu$ M chloroquine), F6H (10  $\mu$ M FCCP for 6 h) and F8H (10  $\mu$ M FCCP for 8 h)

## Discussion

Mitochondria are highly dynamic organelles which form interconnected network (shared common matrix) in the cell e.g neuron and help in maintaining efficient ATP production via electron transport chains (17). The need for healthy mitochondria is crucial particularly in neuron due to the fact that mitochondria are the sole source of cellular energy (18). On average, the number of mitochondria per cell is estimated to be around 200 and this increases more towards cells involve in movement e.g. myocytes and neurons (19). Higher mitochondrial fragmentation could be demonstrated in the fibroblasts obtained from patients with Leigh's syndrome (20). Increased expression mitochondrial promoting proteins relative to those promoting fusion was reported in the neurons from mouse model of Alzheimer disease (21). During mitochondrial fission, one daughter mitochondrion usually becomes depolarized (22), fission-induced mitochondrial depolarization. Depolarized below certain degree (22) is required for stabilization of PINK1 on outer membrane of mitochondria and induction of mitochondrial removal via autophagy (23).

Our preliminary data indicated an increase in mitochondrial fission in LHON patient (A3) via morphology-based observation (data not shown). MMP values in the

borderline range were consistently demonstrated in fibroblast from LHON carrier (U3). While MMP of fibroblast from LHON patient exhibited subtle reduction but statistically significance. However, MMP of fibroblast from LHON patients from different family appeared to be normal. This suggested more than one mechanism as a cause of incomplete penetrance seen in LHON disease despite of homoplasmic status.

We have confronted with difficulties in develop unbiased observation of mitophagy. Five methods have been tried and two of them are reliable in our hands. Only colocalization of mitochondrial and lysosome specific dyes were robust enough for high content imaging system (Figure 11) and subsequent image analysis with CellFrofiler 3.0. Increased and decreased mitophagic response was observed in fibroblast with G11778G>A carrier (U3) and patient respectively Figure 12. This notion could be replicated in another experiment (data not shown). Consequently, we hypothesized that diminished mitophagy response in get rid of damaged mitochondria is one of the key mechanism in determining the manifestation of LHON disease.

## Conclusion

1. Sensitive evaluation of mitochondrial membrane potential (MMP) was established—it can detect a small change in MMP upon sensitization with FCCP as low as 0.001  $\mu$ M (conventional method in literature is only sensitive to 0.1  $\mu$ M level) (24).
2. Slightly diminished MMP was shown in LHON patient's fibroblast from family 1 but not from family 79.
3. Mitophagy detection based on colocalization of mitochondrial and lysosome specific dyes was established employing high content imaging system.
4. Diminished mitophagy could be one of the key event in accumulation of damaged mitochondria and the onset of disease In LHON.
5. Unbiased detection of mitochondrial fission is developing to connect key processes—mitochondrial fission-fusion, mitochondrial bioenergetics (MMP) and mitochondrial quality control (mitophagy).

## Outcome

Publication: None

Student: 3 master degree students

Grant: Health System Research Institute (2019-2020)

## Computer softwares

jamovi project (2018). jamovi (Version 0.9) [Computer Software]. Retrieved from <https://www.jamovi.org>

R Development Core Team (2008). R: A language and environment for statistical computing. R Foundation for Statistical Computing, Vienna, Austria. ISBN 3-900051-07-0, URL <http://www.R-project.org>

Carpenter AE, Jones TR, Lamprecht MR, Clarke C, Kang IH, Friman O, Guertin DA, Chang JH, Lindquist RA, Moffat J, Golland P, Sabatini DM (2006) CellProfiler: image analysis software for identifying and quantifying cell phenotypes. *Genome Biology* 7:R100. PMID: 17076895

## References

1. Huoponen K, Vilkkilä J, Aula P, Nikoskelainen EK, Savontaus ML. A new mtDNA mutation associated with Leber hereditary optic neuropathy. *American journal of human genetics*. 1991;48(6):1147-53.
2. Wallace DC, Singh G, Lott MT, Hodge JA, Schurr TG, Lezza AM, et al. Mitochondrial DNA mutation associated with Leber's hereditary optic neuropathy. *Science* (New York, NY). 1988;242(4884):1427-30.
3. Johns DR, Neufeld MJ, Park RD. An ND-6 mitochondrial DNA mutation associated with leber hereditary optic neuropathy. *Biochemical and biophysical research communications*. 1992;187(3):1551-7.
4. Bi R, Logan I, Yao Y-G. Leber Hereditary Optic Neuropathy: A Mitochondrial Disease Unique in Many Ways. In: Singh H, Sheu S-S, editors. *Pharmacology of Mitochondria*. Cham: Springer International Publishing; 2017. p. 309-36.
5. Chuenkongkaew WL, Lertrit P, Poonyathalang A, Sura T, Ruangvaravate N, Atchaneeyasakul L, et al. Leber's hereditary optic neuropathy in Thailand. *Jpn J Ophthalmol*. 2001;45(6):665-8.
6. Phasukkijwatana N, Chuenkongkaew WL, Suphavilai R, Luangtrakool K, Kunhapan B, Lertrit P. Transmission of heteroplasmic G11778A in extensive pedigrees of Thai Leber hereditary optic neuropathy. *Journal Of Human Genetics*. 2006;51:1110.
7. Neupane P, Bhujju S, Thapa N, Bhattarai Hitesh K. ATP Synthase: Structure, Function and Inhibition. *Biomolecular Concepts* 2019. p. 1.
8. Alers S, Löffler AS, Wesselborg S, Stork B. Role of AMPK-mTOR-Ulk1/2 in the regulation of autophagy: cross talk, shortcuts, and feedbacks. *Molecular and cellular biology*. 2012;32(1):2-11.
9. Fayzulín RZ, Pérez M, Kozhukhar N, Spadafora D, Wilson GL, Alexeyev MF. A method for mutagenesis of mouse mtDNA and a resource of mouse mtDNA mutations for modeling human pathological conditions. *Nucleic acids research*. 2015;43(9):e62.
10. Yen MY, Lee JF, Liu JH, Wei YH. Energy charge is not decreased in lymphocytes of patients with Leber's hereditary optic neuropathy with the 11,778 mutation. *Journal of neuro-ophthalmology : the official journal of the North American Neuro-Ophthalmology Society*. 1998;18(2):84-5.

11. Korsten A, de Coo IF, Spruijt L, de Wit LE, Smeets HJ, Sluiter W. Patients with Leber hereditary optic neuropathy fail to compensate impaired oxidative phosphorylation. *Biochimica et biophysica acta*. 2010;1797(2):197-203.
12. Heytler PG. Uncouplers of oxidative phosphorylation. *Methods in enzymology*. 1979;55:462-42.
13. Mauthe M, Orhon I, Rocchi C, Zhou X, Luhr M, Hijlkema KJ, et al. Chloroquine inhibits autophagic flux by decreasing autophagosome-lysosome fusion. *Autophagy*. 2018;14(8):1435-55.
14. Ouhabi R, Boue-Grabot M, Mazat JP. Mitochondrial ATP synthesis in permeabilized cells: assessment of the ATP/O values in situ. *Analytical biochemistry*. 1998;263(2):169-75.
15. Manfredi G, Yang L, Gajewski CD, Mattiazzi M. Measurements of ATP in mammalian cells. *Methods (San Diego, Calif)*. 2002;26(4):317-26.
16. Kogure T, Kawano H, Abe Y, Miyawaki A. Fluorescence imaging using a fluorescent protein with a large Stokes shift. *Methods (San Diego, Calif)*. 2008;45(3):223-6.
17. Burté F, Carelli V, Chinnery PF, Yu-Wai-Man P. Disturbed mitochondrial dynamics and neurodegenerative disorders. *Nature Reviews Neurology*. 2014;11:11.
18. Martin LJ. Chapter 11 - Biology of Mitochondria in Neurodegenerative Diseases. In: Teplow DB, editor. *Progress in Molecular Biology and Translational Science*. 107: Academic Press; 2012. p. 355-415.
19. Westermann B. Bioenergetic role of mitochondrial fusion and fission. *Biochimica et Biophysica Acta (BBA) - Bioenergetics*. 2012;1817(10):1833-8.
20. Capaldi RA, Murray J, Byrne L, Janes MS, Marusich MF. Immunological approaches to the characterization and diagnosis of mitochondrial disease. *Mitochondrion*. 2004;4(5):417-26.
21. Calkins MJ, Manczak M, Mao P, Shirendeb U, Reddy PH. Impaired mitochondrial biogenesis, defective axonal transport of mitochondria, abnormal mitochondrial dynamics and synaptic degeneration in a mouse model of Alzheimer's disease. *Human molecular genetics*. 2011;20(23):4515-29.
22. Twig G, Elorza A, Molina AJA, Mohamed H, Wikstrom JD, Walzer G, et al. Fission and selective fusion govern mitochondrial segregation and elimination by autophagy. *The EMBO journal*. 2008;27(2):433-46.
23. Narendra DP, Jin SM, Tanaka A, Suen DF, Gautier CA, Shen J, et al. PINK1 is selectively stabilized on impaired mitochondria to activate Parkin. *PLoS Biol*. 2010;8(1):e1000298.
24. Brennan JP, Berry RG, Baghai M, Duchen MR, Shattock MJ. FCCP is cardioprotective at concentrations that cause mitochondrial oxidation without detectable depolarisation. *Cardiovascular research*. 2006;72(2):322-30.